PROTOTYPE PULSE MODULATOR FOR HIGH-POWER KLYSTRON IN PLS LINAC

S. H. Nam, J.S. Oh, M. H. Cho, and W. Namkung

Pohang Accelerator Laboratory
Pohang Institute of Science and Technology
P. O. Box 125
Pohang, 790-600 KOREA

ABSTRACT

Pohang Accelerator Laboratory (PAL) is constructing a 2 GeV electron linac. To achieve the final electron energy, it employs total eleven units of high power klystron (65 or 80 MW) and pulse modulator (>150 MW) as RF power source. PAL is now constructing 200 MW modulators (400 kV, 4.4 μs flat top, 800 Ω load). A prototype 150 MW modulator (350 kV, 3.5 μs flat top, 840 Ω load) is already constructed and under operation with a dummy load. Required parameters of modulators and construction of the prototype are presented.

INTRODUCTION

The final energy goal of Pohang Light Source (PLS) electron linac is 2 GeV. To achieve the final energy, eleven high power klystron and modulator units as well as 10 SLED cavities [1] are necessary with somewhat modest energy margin. The required peak power of modulator is greater than 150 MW. PLS constructed a 150 MW prototype pulse modulator. The unit is now under operation with a water dummy load. The final main modulator, which has a 200 MW peak power, is designed and under construction. This paper briefly describes required operational parameters of both 150 and 200 MW modulators according to the current linac specification and designed parameters of the current modulators. In addition this paper presents the construction and experimental results of the 150 MW prototype modulator.

MODULATOR AND LOAD SPECIFICATION

To achieve the final 2 GeV electron energy of linac, RF output power of klystron load should be greater than 65 MW. There are only two known manufacturers that produce such klystron tubes: Stanford Linear Accelerator Center (SLAC) in USA and Toshiba in Japan. The required modulator peak power is 150 MW for SLAC 5045 tube and 200 MW for Toshiba E3712 tube. Table 1 summarizes required and designed parameters of modulators. In the table 1, the designed average power of 200 MW modulator has some margin from the required one. This margin allows full power operation of SLAC tube with some modification in the modulator circuit and also any future energy upgrade.

TABLE 1
MAIN PARAMETERS OF MODULATOR

	150 MW FOR SLAC TUBE	200 MW FOR TOSHIBA TUBE
Peak Power (MW)	150	200
Ave. Power (kW) - Required - Designed	 66 66	 97 289
Peak Out. Voltage (kV)	350	400
Repetition Rate (PPS) - Required - Designed	 10 to 60 60	 10 to 60 180
Equi. Pulse Width (μS)	6.56	7.5
Flat Top Pulse Width (< +/- 0.5 %) (μS)	3.5	4.4
PFN Impedance (Ω)	3.73	2.8
Thyratron - Peak Power (MW) - Ave. Power (kW)	ITT F-241 125 200	ITT F-303 200 200

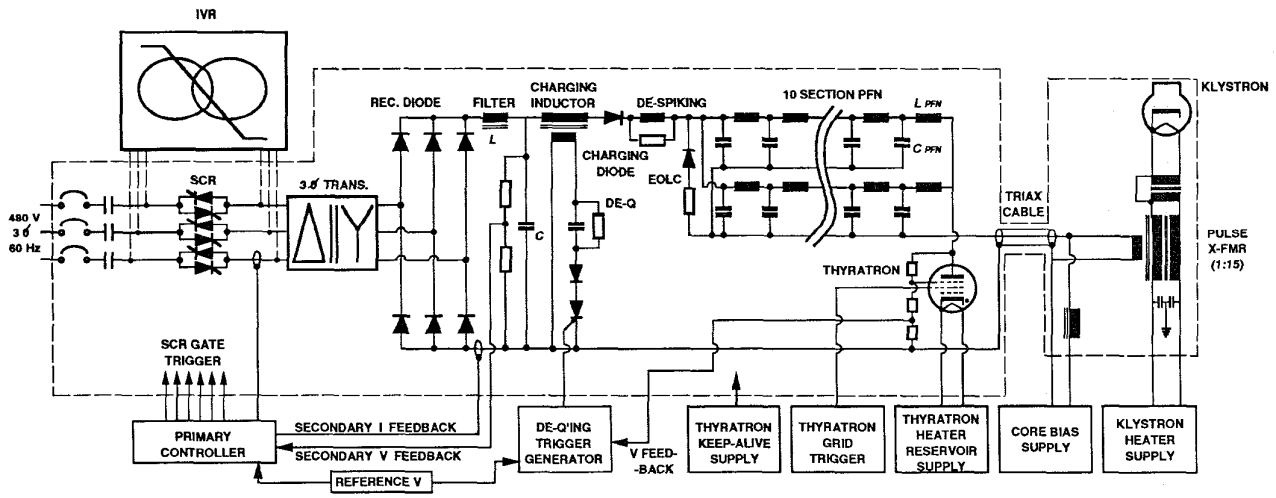

Figure 1 Simplified circuit diagram of modulator.

150 MW PROTOTYPE MODULATOR

In order to realize the specifications of 150 MW modulator given in Table 1, a line type is selected because of its well established technology and reliability proven in many other world's linac facilities [2,3,4]. A simplified PLS modulator circuit diagrams is given in Figure 1. It mainly consists of a charging system, a discharging circuit, a pulse transformer assembly, and a load.

CHARGING

Resonant charging system is adopted to transfer charge from DC power supply to PFN capacitors. The main components of charging system are a DC power supply, a charging inductor, a charging diode assembly, a de-spiking circuit, and PFN capacitors. A De-Q'ing circuit is also employed for fine regulation of charging voltage on PFN capacitors. Key specifications of charging components are listed in Table 2.

TABLE 2
SPECIFICATION OF MAIN CHARGING COMPONENTS

DC HV Power Supply	25 kV , 3 A av. <3 % Regulation 14.1 μF Filter Capacitor
Charging Inductor	2.4 H Primary 1:25 Turn Ratio
Charging Diode	115 kV, 40 A Total. 72 Diodes in Series. Snubber: 330 kΩ, 2.2 nF (Parallel)
De-Spiking	R: 2 kΩ, L: 14 mH in Parallel
Total PFN Capacitance	0.88 μF
Charging Time	4.57 ms

The power supply is a conventional, three-phase full-wave bridge dc supply with choke input filter. For controlling of 3-phase primary power of 66 kW average , both an induction voltage regulator (IVR) and a phase-control system with six SCRs are tried during testing of the 150 MW modulator. The phase controller is more effective in terms of cost, space, and controllability. Therefore, the phase-control charging scheme is selected for control of full 3-phase primary power. The rectifier transformer has delta primary and wye secondary. A three phase, full-wave rectifier assembly is connected to the transformer secondary. The assembly has six stacks of diodes. Each diode stack has 96 diodes connected in series. Each diode has 1600 V peak inverse voltage (PIV) and 16 A average current capability. In Figure 1, the inductance of the filter choke is 5 H, and the capacitance of the filter capacitor is 14.1 μF. Since the PFN capacitance is much smaller than the filter capacitance, the charging time T_c and the PFN charging voltage V_{PFN} can be approximated as follows;

$$T_c = \frac{\pi}{\omega_c} = \pi\sqrt{L_c C_{PFN}} ,$$

$$V_{PFN} = V_{DC}(1-\cos\omega_c t) ,$$

where, ω_c = Resonant charging frequency,
L_c = Inductance of the charging inductor,
C_{PFN} = Total PFN capacitance, and
V_{DC} = DC Power supply voltage.

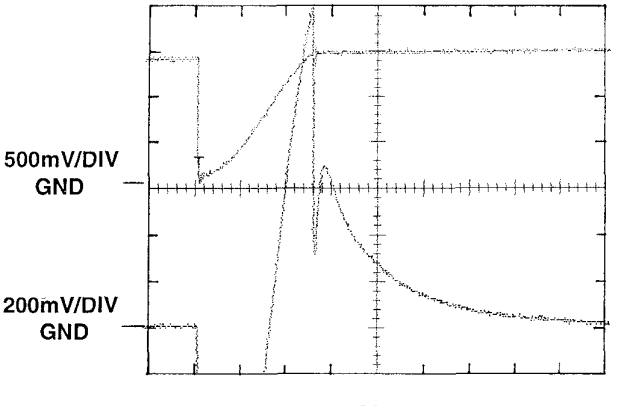

Figure 2 PFN charging voltage with ~7.9 kV peak (upper) and voltage across a resonant charging inductor secondary with ~ 140 V positive peak (lower). The second positive peak in the lower signal indicates ~ 9.5 % De-Q'ing. Only half of the PFN capacitors are used during the test.

In the present system, the droop is measured to be less than 1 % in 10 PPS, and 0.2 % in 60 PPS operation. Since the droop rate of the PFN charging voltage is nearly constant at a fixed PRR, the pulse-to-pulse load voltage does not vary because of the droop. Required pulse-to-pulse load voltage variation is less than 0.5 %. A De-Q'ing circuit is employed to accomplish the required regulation. When V_{PFN} reaches desired level, the De-Q'ing SCR is triggered to remove energy remained in the charging inductor. Regulation of the De-Q'ing is set from 2 % to 5 % of the full PFN charging voltage. The leakage inductance of charging inductor is minimized (0.02 H maximum) to reduce the residual energy remained in the leakage and not extracted by the De-Q'ing action. The De-Q'ing is consisted of an SCR switch and a diode in a series connection of RC parallel network in which R and C are respectively 2 Ω and 50 μF. In Figure 2, an example of De-Q'ing waveform along with V_{PFN} signal is shown. Only half of the PFN capacitors are used for the test in Figure 2. The De-Q'ing should satisfy the following two most important conditions: (1) The peak voltage across primary of charging inductor during De-Q'ing should be smaller than the PFN charging voltage. (2) The energy in the charging inductor should be removed by the De-Q'ing action before starting next charging cycle. Various values of R and C in the De-Q'ing are tried to find optimum value. Near critical-damping seems to be the best for the operation because of no oscillation and fast decay in the tail of De-Q'ing waveform. For the operation of 150 MW modulator, a selectable range of R and C is found to be wide because of the given long time period between charging intervals(60 PPS). Usable ranges of R and C in 150 MW operation are 2 to 6 Ω and 50 to 150 μF. A charging diode assembly is connected in series with the charging inductor as shown in Figure 1. The charging diode assembly holds PFN voltage at about twice of V_{DC} after completion of charging. The de-spiking network in Figure 1 protects charging inductor and diode assembly from any voltage and current spikes.

DISCHARGING CIRCUIT

Main elements of the discharging circuit are capacitors and variable inductors of PFN, a high power thyratron switch, a triaxial cable, a pulse transformer, a load, and the end of line clipper (EOLC) circuit. Type E Guillemin networks is selected as a PFN network because of its easiness of construction and flexibility of impedance tuning [5]. The impedance of PFN is 3.73 ohm which

is decided by the load impedance reflected to the primary side of the pulse transformer at the maximum operating voltage. The PFN impedance Z_{PFN} is

$$Z_{PFN} = \sqrt{\frac{L_{PFN}}{C_{PFN}}}$$

where, L_{PFN} = Total PFN inductance, and
C_{PFN} = Total PFN capacitance.

Equivalent pulse-width τ of the desired output voltage has the following relationship with PFN parameters;

$$\tau = 2\sqrt{L_{PFN}C_{PFN}}$$

By considering system risetime of 0.8 μS and flattop pulse-width of 3.5 μS as given in Table 1, the number of PFN sections and the equivalent pulse-width are decided as 10 sections and 6.56 μs, respectively. The PFN configuration is 2-parallel 10-section network. Values of L and C for each section are calculated to be 2.45 μH and 0.044 μF, respectively. The tuning of pulse top flatness is done by varying inductance of each section. The PFN inductance of each section is not fixed, but variable value. The maximum inductance obtainable from the tunable inductor is about 4.5 μH. With the optimized value of PFN parameters, the desired pulse is generated by externally triggering a high power switch. The ITT F-241 thyratron is selected as the switch for 150 MW modulator to have reliable operation and longer lifetime of the discharging circuit. The reliability and lifetime of the F-241 thyratron has already been proven in current SLAC modulators with thousands of operational hours. Table 3 shows main parameters of ITT F-241 thyratron.

TABLE 3
ITT F-241 THYRATRON SPECIFICATIONS

Max. Peak Power [MW]	125 (145)
Max. Average Power [kW]	200 (66)
Max. Peak Anode V, Forward [kV]	50 (47)
Max. Peak Anode Current [kA]	10 (6.23)
Max. Average Anode Current [A]	8 (2.42)
Max. RMS Anode Current [A]	200 (123)
Max. Heating Factor [pb = epy x ib x prr]	400 x 10^9 (28 x10^9)

The values given in parentheses of Table 3 are operating values of 150 MW modulator. Low duty factor of the modulator is making up the peak power capability of the thyratron higher than the specified value. The energy charged in PFN is transferred to load via the pulse transformer shown in Figure 1. The pulse transformer (Stangenese Model SI-6833) will be positioned in an aluminum tank and immersed in a high voltage insulating mineral oil. The PFN in the modulator cabinet and pulse transformer in the oil tank will be connected by using a triaxial cable assembly (Insulation Design Model 2035). For the on-going preliminary test, a plastic oil tank and an ordinary high-voltage 50 ohm coaxial cable (RG 117) are in temporary use. The turn ratio of the pulse transformer is 1:15. The transformer steps voltage up to 350 kV required. Voltage and current of load are measured by a ~10,000:1 capacitive voltage divider (Stangenese Model SI-6843) and a 0.1 V/A pulse current transformer (Stangenese Model SI-3680). Figure 3 shows voltage and current signals of the water dummy load. Peak voltage level

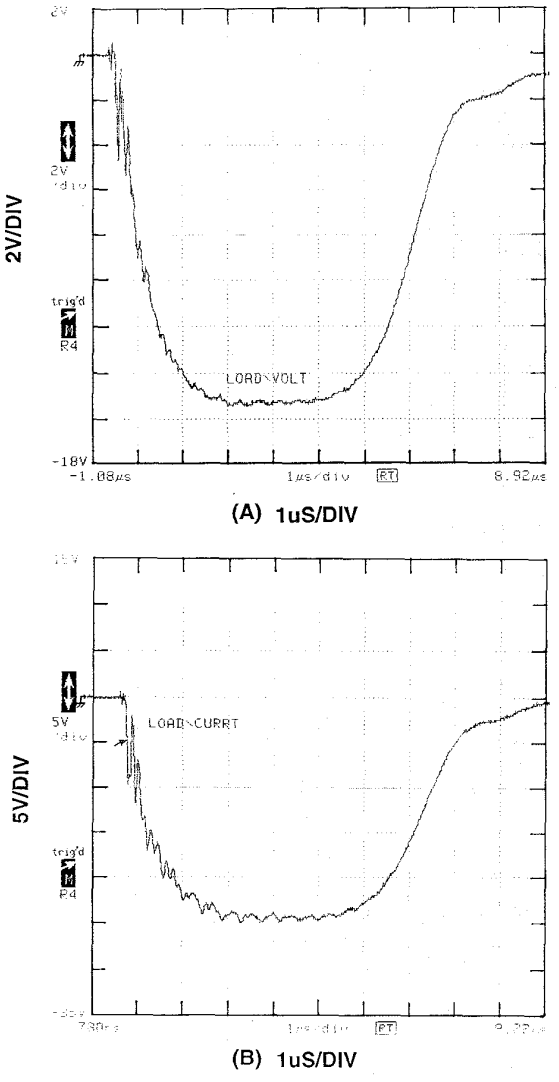

Figure 3 (A) Voltage across a water dummy load: ~200 kV peak, 6.2 μs FWHM.
(B) Current through a water dummy load: ~245 A peak.

is ~200 kV with 6.2 μs FWHM. The current is about 245 A peak. The load impedance is calculated to be 816 Ω (3.63 Ω in the primary). The measured rise and fall time of the pulse are about 1.4 μs and 2.3 μs, respectively. The measured flat-top width is 2.3 μs. This rather slow rise and fall of load waveform is due to the pulse cable and pulse tank which is in temporary use. The temporary system has quite large inductance caused by long leads between connections. If load faults or breakdowns in the oil tank occur, the effective load impedance becomes very low. An EOLC circuit is installed to remove excessive negative voltage swing caused by negative impedance mismatch. The negative voltage swing could damage PFN capacitors and the thyratron. A series combination of diodes and a ~4 Ω water resistor is used as the EOLC circuit shown in Figure 1. The EOLC diode assembly has the same configuration and specification as the charging diode except that the connections are made to minimize the system inductance. Since the EOLC current is direct indication of faults, a pulse current

transformer (0.2 V/A, Stangenese Model SI-6838) is installed to continuously monitor the current.

IMPEDANCE MISMATCH

Klystron load current I_k has the following dependence on applied beam voltage V_B;

$$I_k = k\, V_B^{3/2}$$

where, k = Perveance of the klystron load
= 2 x 10^{-6} for SLAC 5045.

The initial beam voltage peak seen at the primary of the pulse transformer V_{Li} is

$$V_{Li} = V_{PFN}\frac{Z_L}{Z_L+Z_{PFN}} = \frac{V_{PFN}}{1+n^{5/2}kZ_{PFN}\sqrt{V_{Li}}}$$

where, Z_L = Load impedance at transformer primary,
n = Turn ratio of pulse transformer,
Z_{PFN} = PFN Impedance, and
V_{PFN} = PFN charging voltage.

Impedance matching condition is closely satisfied only with full operating voltage of the modulator. Thus, impedance mismatch presents when the applied voltage across load is lower than the full value. If impedance mismatch exists, reflected voltage peaks appear after the main pulse V_{Li}. The following equation shows the first reflected voltage amplitude V_{R1} that follows the main pulse V_{Li};

$$V_{R1} = V_{Li} - \frac{2n^{5/2}kZ_{PFN}V_{Li}^{3/2}}{1+n^{5/2}kZ_{PFN}\sqrt{V_{Li}}}$$

By plotting relations of V_{PFN}, V_{Li}, and V_{R1}, one can find that the impedance mismatch is positive at the applied voltage lower than full operating value. The maximum reflection occurs when V_{Li} equals to 8.6 kV, and the amplitude of V_{R1} is 2 kV. To operate the modulator in the whole voltage range, the thyratron switch should be able to recover from the prolonged conduction due to the positive mismatch before fully developing the next charging cycle. Assuming that the thyratron recovers when voltage across it is lower than 200 V, the recovery time of thyratron in the worst mismatch condition is calculated to be about 25 μs. During this time, the charging current flow is not yet developed appreciably to affect the thyratron recovery. Because of this result, the modulator with a klystron load is selected to operate in a positive mismatch mode. This implies that, even in the full applied voltage, there exists certain positive reflection (less than 5 %). A main advantage of this mode of operation is a longer switch lifetime by reducing the thyratron anode dissipation.

SYSTEM CONTROL AND INTERLOCK

A main control point of the 150 MW modulator is a high voltage level. As shown in Figure 1, one reference voltage source with an excellent voltage regulation (<0.01%) is used to decide the IVR position or SCR firing angle, and De-Q'ing SCR trigger level. The IVR position or the firing angle of SCR phase charging decide V_{DC}. The De-Q'ing trigger level decides V_{PFN}. One reference control voltage ensures the De-Q'ing operation with a constant percentage of V_{PFN}, which is a direct function of V_{DC} as described in previous sections. Various interlocks are used in the 150 MW modulator. The interlock system has two groups; static and dynamic. The static interlocks stop the modulator operation as soon as any static fault condition activates. When dynamic system faults are detected, the modulator operation is halted for a moment (1 to 8 seconds variable) and recovers automatically. This retrial is done several times (1 to 8 trials variable) and shuts the system down after the number of faults exceeds the trial setting. An external reset is necessary to operate the modulator again. The dynamic interlock system includes a beam overvoltage, a beam overcurrent, an EOLC overcurrent, a DC high voltage overcurrent, and a voltage standing wave ratio (VSWR) at the output waveguide of the klystron load. Interlocks directly related to klystron is available, but not connected in the current test setting in which a water dummy load is installed. These interlocks include a load vacuum, and the VSWR.

SUMMARY

Preliminary test of the 150 MW prototype modulator has shown satisfactory performances up to 110 MW even with many temporary components. Full power operation of the modulator will be performed after installing a SLAC 5045 klystron tube, the triaxial cable assembly, the aluminum pulse transformer oil tank, and others. Long term operational characteristics of the modulator will be carefully monitored in order to ensure long and reliable operation of linac after installing the modulator in the facility. Results of the 150 MW klystron and modulator unit operation as well as the construction of 200 MW modulators are subjects to a next paper.

ACKNOWLEDGEMENT

This work is supported by Pohang Steel and Iron Company (POSCO) and the Korean Ministry of Science and Technology (MOST). The authors wish to express our appreciation for the effort provided by N. P. Park, S. S. Park, S. W. Park, Y. K. Son, S. D. Jang, K. T. Lee, S. H. Kim, K. Choi, H. S. Bang, and W. B. Chung.

REFERENCE

1. Z.D. Farkas, H.A. Hogg, G.A. Loew, P.B. Wilson, "Recent Progress on SLED, The SLAC Energy Doubler," IEEE Tran. on Nuclear Science, NS-22, 3, 1975, pp 1299-1302.
2. R.B. Neal, ed, The Stanford Two-Mile Accelerator, Q.A. Benjamin, New York, 1968.
3. T. Shidara et al., "Klystron Modulator for the KEK 2.5 GeV Linac," Nucl. Instrum. and Methods in Phys. Res., A279, 1989, pp 423-432.
4. P. Pearce, S. Hutchins, "Present Performance of the LEP Pre-Injector Klystron Modulators and the Impact of a Proposed Upgrade," IEEE Conf. Records of the 19th Power Modulator Symp., San Diego, CA., 1990, pp 124-129.
and many other references are available.
5. G. N. Glasoe and J. V. Lebacqz, Pulse Generators, McGraw-Hill, 1948, Chapter 6.